PCCP

Experimental determination of singly scattered light close to the critical point in a polystyrene–cyclohexane mixture

Jörg-Michael Schröder,[a] Simone Wiegand,*[b] Lisa B. Aberle,[c] Malte Kleemeier[a] and Wolffram Schröer[a]

[a] *Institut für Anorganische und Physikalische Chemie, Universität Bremen, Leobener Str. NW2 28334 Bremen, Germany*
[b] *Max-Planck-Institut für Polymerforschung, Ackermannweg 10, 55128 Mainz, Germany*
[c] *Fraunhofer-Institut für Fertigungstechnik und angewandte Materialforschung, Wiener Str. 12, 28359 Bremen, Germany*

Received 14th April 1999, Accepted 1st June 1999

In turbid media the presence of multiple scattering constitutes a major complication for the analysis of the intensity and of the intensity correlation functions of the scattered light. The 3D-cross-correlation technique provides an effective means to determine the single scattering intensity and to suppress the influence of multiple scattering to the time dependence of correlation functions. The technique is applied to study the temperature dependence of the critical fluctuations of a solution of polystyrene ($M_w = 1.11 \times 10^5$ g mol^{-1}) in cyclohexane. We show that the single scattering intensity determined for a scattering angle of $\theta = 90°$ can be described by the Ornstein–Zernike function over the entire temperature range of 313.15–293.49 K. Good agreement between experiment and Monte Carlo simulations of the scattering processes is found for the ratio of singly scattered light to the total scattering intensity.

1 Introduction

One of the most striking effects close to the critical point of mixtures is the enormous increase of the order parameter fluctuations. These order parameter fluctuations have been studied in binary mixtures and polymer solutions.[1] It is generally accepted that all fluid systems belong to the same universality class of the three-dimensional Ising model characterized by a set of critical exponents.[2] The divergence of the correlation length is described by the asymptotic power law $\xi = \xi_0 \varepsilon^{-\nu}$, with the reduced temperature $\varepsilon = (T - T_c)/T_c$ and the critical exponent $\nu = 0.63$ of the 3D-Ising model.

Dynamic and static light scattering is a frequently used method to study the critical behavior of static and transport properties in fluids and fluid mixtures. The critical slowing down of the order parameter fluctuations can be detected by measuring the time dependent correlation function of the scattered photons, while an increase of the concentration fluctuations manifests itself in an increase of the scattering intensity. Close to the critical point the interpretation of the light scattering results is complicated by multiple scattering. Recent measurements on polydisperse polymer solutions of polystyrene in cyclohexane and methylcyclohexane have been reported,[3] which, however, could only be analyzed for reduced temperatures $\varepsilon \geqslant 3.4 \times 10^{-4}$ due to the presence of multiple scattering closer to the critical point.

Several attempts have been made to determine the amount of multiply scattered light theoretically[4–6] or by Monte Carlo simulations.[7] The theoretical method by Shanks and Sengers[4] calculates the double-scattering contributions in critically opalescent samples for which the angle dependent scattering cross section is given by the Ornstein–Zernike equation. An extension of the theory to higher orders of multiple scattering becomes very complicated due to manifold integrals. Under the conditions of multiple scattering a direct simulation of the scattering intensity by Monte Carlo simulations seems to be a more promising aproach.[7] It is worth pointing out that the theoretical and simulation approaches require a precise knowledge of the experimental constraints.

Applying cross-correlation techniques it is possible to suppress the contributions of multiply scattered light to the time correlation functions experimentally. Furthermore it could be shown in some experiments that the analysis of the amplitude of the cross-correlation functions enables one to determine the single scattering intensity.[8,9] Different techniques have been proposed and successfully applied.[8–14]

The basic idea of the so-called two-color coding experiment and the three-dimensional set-up is similar.[15] In both set-ups the scattering experiment is done twice in the same scattering volume with identical resulting scattering vectors $q_{1,2} = (4\pi n_{1,2}/\lambda_{1,2})\sin(\theta_{1,2}/2)$ with n and λ denoting the refractive index and the wavelength, respectively. In the two color-coding technique this is achieved in a planar geometry by choosing the scattering angle $\theta_{1,2}$ for both colors in such a way that the same scattering vector $q_1 = q_2 = q$ results. In the 3D-set-up the same scattering vectors are obtained by rotating the initial and final wave vector pairs by a small angle about the common scattering vector. In both experiments the scattered light recorded by the two detectors is cross-correlated. It turns out that only the light which is scattered once on its way to the detector belongs to the same scattering vector and is correlated, while the resulting scattering vectors of the multiply scattered light add up differently for the distinct paths on the way to the detector and, therefore, are statistically independent. While both those experiments use the circumstance that the scattering behavior is determined by the scattering vector, the one-beam set-up suggested by Meyer *et al.*[12] uses the fact that the singly scattered light results in a larger coherence area. By placing the two detectors at the edge of the coherence area almost only singly scattered light is correlated.

A different design of the same idea has been realized by Nobbmann *et al.*[13] and the theoretical background of the mechanism of multiple scattering suppression has been discussed in detail by Lock.[16] Additionally Ovod[17] simulated the one-beam cross-correlation experiment and determined the optimal displacement of the detectors. The 3D-cross-correlation method so far successfully tested by measuring the static and dynamic light scattering properties of highly turbid latex suspensions will be applied for the first time to study the temperature dependent critical fluctuations of the local composition of a solution of polystyrene in cyclohexane. The system has an upper critical solution point. We investigate a temperature range of 20 K down to 2×10^{-3} K above T_c. This range corresponds to reduced temperatures ε of 6.8×10^{-6} to 0.067 with $T_c = 293.492$ K. We determine the intensity of the singly scattered light and show that it is perfectly described by the Ornstein–Zernike function in the entire temperature range. Even very close to the critical point, where the turbidity reaches a value of 2.4 cm^{-1}, no deviations are noticeable. In addition, we compare the intercept or amplitude of the cross-correlation function with the ratio of singly scattered photons to total scattered photons obtained from a Monte Carlo simulation of the multiple scattering processes. The agreement between experiment and simulation is very good.

2 Experimental

2.1 Sample preparation and apparatus

We used polystyrene with a molecular weight $M_w = 1.11 \times 10^5$ g mol^{-1} and $M_w/M_n = 1.061$, where M_w is the weight-average molecular weight and M_w/M_n is the ratio of weight- to number-averaged molecular weights. The polystyrene was synthesized by anionic polymerization using tetrahydrofuran as solvent and butyllithium as starter. The polymer was precipitated in an excess of methanol. As it is known[18] that the critical temperature depends strongly on the water content, we dried the polystyrene for two weeks in a desiccator with phosphorus pentoxide. The cyclohexane (Fluka, puriss) was used without further purification as the specified water content is below 0.005%.

The sample preparation was carried out in a dry box, which was flushed with argon and maintained at a slight overpressure. The cells were dried for one week at 130 °C and transferred to the dry box. The solutions were passed through a membrane filter (Roth, 0.2 μm pore size) in cylindrical sample cells with an inner diameter of 1 cm. To determine the critical weight fraction we flame sealed several samples of various concentration. The critical mass fraction $y_c = 0.118 \pm 0.001$ was determined according to the equal volume criterion by measuring the ratio of phase volumes 20 mK below the phase separation temperature. The system has an upper critical point at the critical temperature $T_c = 293.492 \pm 0.002$ K.

Construction and performance of our 3D-cross-correlation apparatus has been described in detail elsewhere.[9,19] The main modification of the set-up for this work is the improved temperature control of the sample cell, which is immersed in a glass cylinder with an inner diameter of 9.5 cm. To minimize reflection losses we used silicon oil (Serva, DC200, 10 cSt) as bath liquid, which was stirred continuously to avoid temperature gradients. To achieve a temperature stability of $\Delta T = \pm 2$ mK we used two stage heating. The intensity of the incoming and transmitted beam was recorded by two photodiodes. This allowed the control of the laser intensity fluctuations and correction of the scattered intensity for turbidity losses. The scattering intensity at 90° is measured by a double photomultiplier unit.

2.2 Procedure and data analysis

The normalized 3D-cross-correlation function of the scattered light intensity $I(t)$ is given by[20]

$$C(t) = \frac{\langle I_A I_B \rangle}{\langle I \rangle^2} = 1 + |R_\tau \cdot G(t)|^2 \quad (1)$$

The time averaged intensity $\langle I \rangle$ is given by the geometric mean value $\langle I \rangle = \sqrt{\langle I_A \rangle \langle I_B \rangle}$, with $\langle I_A \rangle$ and $\langle I_B \rangle$ the measured scattering intensities at the detectors A and B, respectively. $G(t)$ is the normalized correlation function of the electric field of the singly scattered light. If $R_{\tau \to 0}$ denotes the amplitude for nearly transparent media, the normalized amplitude $R_* = R_\tau / R_{\tau \to 0}$ is equal to the intensity ratio of single scattering to multiple-scattering contributions. In this way the intensity of the singly scattered light $\langle I_s \rangle$ can be obtained by

$$\langle I_s \rangle = R_* \cdot \langle I \rangle. \quad (2)$$

Investigating standard monodisperse latex samples, we have verified that the amplitude does not change with temperature in the range from 20–40 °C at a scattering angle of $\theta = 90°$. Therefore, we conclude that the temperature variation of the refractive index in this region causes no noticeable change of size and position of the scattering volume in our set-up. This fact enables us to compare the data at different temperatures.

The single scattering intensity i_{90} of a critical binary mixture can be analyzed in the frame work of the Ornstein–Zernike theory.[21] According to this theory i_{90} can be written in the form

$$i_{90} = A(1 + \varepsilon) \frac{\varepsilon^{-(2-\eta)\nu}}{1 + (q\xi_0 \varepsilon^{-\nu})^2} + B. \quad (3)$$

We used the scaling laws $\chi = \chi_0 \cdot \varepsilon^{-(2-\eta)\nu}$ and $\xi = \xi_0 \cdot \varepsilon^{-\nu}$ for the osmotic susceptibility and correlation length, respectively. The critical exponent η denotes the Fisher exponent. The baseline B accounts for the non-critical scattering contributions caused by the relatively large polymer. The scattering vector is $q = 0.0202$ nm^{-1}. The constant A depends on the properties of the sample and the geometrical constraints of the optical set-up, and can be treated as temperature independent.

In order to obtain the singly scattered light intensity, which can be described by eqn. (3), the count rate N_p measured by the photomultiplier has been corrected for the loss due to turbidity τ and for multiple scatering $R_*(\tau)$.

$$i_{90} = N_p \cdot e^{\tau l} \cdot R_*(\tau) \quad (4)$$

The measured intensity ratio of the transmitted to incoming light intensity $\Re = I_t/I_0$ is related to the sample turbidity by the following equation:

$$\Re = e^{-\tau l} = e^{-(\tau_0 \varepsilon^{-(2-\eta)\nu} f(\alpha) + \tau_b) l} \quad (5)$$

Here $\alpha = 2(2\pi n \xi_0 \varepsilon^{-\nu}/\lambda_0)^2$ with n the refractive index, ξ_0 the correlation-length amplitude, and λ_0 the vacuum wavelength of the laser light. The Ford–Puglielli function[22] is denoted as $f(\alpha)$. The symbol τ_0 represents the critical amplitude of the turbidity and τ_b accounts for some background turbidity contributions. The path length l denotes the distance the beam traversed inside the sample cell on its way to the detector. In our set-up the scattering volume is located in the centre of the cell, therefore $l = 1$ cm. The uncertainty of the scattering intensity is propagated from the uncertainties of the directly measured quantities as described in ref. 22. Additionally, we included the relative error $\delta R_*/R_*$ of the normalized amplitude of the cross-correlation function.

3 Results and discussion

In Table 1 we give the temperatures with the corresponding data for the transmissions $\Re$, for the normalized amplitudes

Table 1 Temperature dependence of transmission $\Re$, normalized amplitude of the cross-correlation function R_*, scattering intensity N_p, and single scattering intensity i_{90} with mean square deviation. N_p denotes the countrate measured by the photomultiplier, which has a mean uncertainty of 0.2%. R_* has been normalized with $R_{\tau\to 0} = 0.3533$ measured at $T = 296.233$ K. i_{90} has been corrected for turbidity losses in the sample and for multiple scattering contributions. The uncertainty σ_{i90} includes temperature fluctuations of $\delta T = 2$ mK, the uncertainty of T_c, of the transmission $\Re$, and of the amplitude R_* of the cross-correlation function. The observed critical temperature is $T_c = 293.492 \pm 0.002$ K. The mean uncertainties of transmission and amplitude of the cross-correlation function are $\sigma_{\Re} = 7.8\%$ and $\sigma_{R_*} = 5\%$.

#	T/K	$\Re$	R_*	N_p/kHz	i_{90}/kHz	$\sigma_{i_{90}}$/kHz
1	313.150	0.9763	—	3.35	3.43	0.27
2	311.150	0.9556	—	3.63	3.80	0.41
3	309.352	0.9423	—	4.00	4.24	0.43
4	307.735	0.9359	—	4.40	4.70	0.55
5	306.281	0.9274	—	4.89	5.27	0.59
6	304.973	0.9255	—	5.44	5.88	0.69
7	303.797	0.9298	—	6.10	6.56	0.75
8	302.740	0.9416	—	6.80	7.22	0.74
9	301.788	0.9562	—	7.66	8.01	0.81
10	300.933	0.9715	—	8.70	8.95	0.84
11	300.164	0.9831	—	9.76	9.93	0.80
12	299.472	0.9942	—	11.01	11.07	0.88
13	298.850	0.9985	—	12.45	12.47	0.94
14	298.291	1.0000	—	14.11	14.11	0.87
15	298.150	0.9989	—	14.45	14.46	1.27
16	297.788	0.9964	—	15.91	15.96	1.12
17	297.335	0.9890	—	17.69	17.89	1.06
18	297.316	0.9874	—	17.90	18.13	1.80
19	296.928	0.9865	—	19.93	20.20	1.13
20	296.632	0.9892	—	22.11	22.36	1.57
21	296.562	0.9818	—	22.28	22.69	1.29
22	296.233	0.9775	1.0000	25.10	25.68	1.65
23	296.071	0.9846	0.9778	27.73	27.54	2.50
24	295.938	0.9742	0.9974	28.81	29.50	1.65
25	295.671	0.9656	0.9980	32.35	33.43	2.06
26	295.612	0.9885	0.9891	34.08	34.10	2.00
27	295.432	0.9560	0.9964	36.21	37.74	2.31
28	295.235	0.9627	0.9906	42.04	43.26	2.43
29	295.217	0.9470	0.9949	40.91	42.97	2.59
30	295.023	0.9371	0.9909	45.90	48.54	3.25
31	294.926	0.9434	0.9854	50.99	53.27	3.06
32	294.849	0.9267	0.9881	51.49	54.90	3.93
33	294.693	0.9129	0.9841	58.02	62.55	3.88
34	294.673	0.9187	0.9792	61.31	65.34	3.58
35	294.552	0.9045	0.9780	64.73	69.99	4.47
36	294.465	0.8876	0.9725	72.88	79.85	4.86
37	294.425	0.8848	0.9815	72.02	79.89	4.66
38	294.312	0.8639	0.9690	80.31	90.08	6.18
39	294.295	0.8532	0.9664	85.41	96.75	6.42
40	294.209	0.8394	0.9657	90.38	103.99	6.24
41	294.155	0.8154	0.9576	98.58	115.77	8.09
42	294.117	0.8110	0.9644	99.25	118.02	7.42
43	294.041	0.7737	0.9493	111.78	137.14	8.15
44	294.034	0.7812	0.9550	109.20	133.49	8.37
45	293.960	0.7446	0.0503	121.30	154.80	8.93
46	293.947	0.7265	0.9353	125.01	160.94	9.10
47	293.893	0.7081	0.9299	131.76	173.02	9.87
48	293.870	0.6761	0.9164	138.10	187.19	11.01
49	293.833	0.6741	0.9217	138.52	189.39	12.83
50	293.807	0.6298	0.9055	148.00	212.79	13.12
51	293.779	0.6265	0.9045	149.34	215.61	12.93
52	293.755	0.5836	0.8805	157.04	236.97	15.12
53	293.730	0.5782	0.8840	157.91	241.41	14.91
54	293.713	0.5501	0.8621	161.45	253.03	16.82
55	293.686	0.5314	0.8706	163.45	267.76	17.37
56	293.678	0.5153	0.8480	164.29	270.37	19.00
57	293.650	0.4769	0.8259	167.67	290.39	20.38
58	293.647	0.4761	0.8354	168.33	295.37	20.31
59	293.626	0.4428	0.7989	167.65	302.48	23.50
60	293.611	0.4195	0.7948	168.63	319.48	23.42
61	293.607	0.4111	0.7713	167.52	314.30	26.37
62	293.591	0.3860	0.7694	167.25	333.41	27.01
63	293.580	0.3559	0.7513	167.15	352.87	28.71
64	293.578	0.3569	0.7340	165.77	340.90	46.10
65	293.568	0.3163	0.6930	163.40	357.96	31.59
66	293.559	0.3100	0.6895	162.84	362.20	37.35
67	293.552	0.2809	0.6630	160.09	377.87	46.65
68	293.551	0.2876	0.6663	160.32	371.39	35.80
69	293.546	0.2638	0.6277	158.27	376.55	59.29
70	293.542	0.2474	0.6124	155.98	386.08	42.62
71	293.538	0.2431	0.5979	154.40	379.73	44.43
72	293.535	0.2382	0.5914	153.02	379.86	45.06
73	293.532	0.2417	0.6133	153.06	388.38	55.36
74	293.530	0.2152	0.5503	149.72	382.95	59.20
75	293.528	0.2271	0.5601	150.46	371.14	54.76
76	293.526	0.2295	0.5974	150.76	392.36	53.77
77	293.525	0.2207	0.5979	150.93	408.84	50.99
78	293.524	0.2069	0.5466	147.84	390.54	69.62
79	293.522	0.2178	0.5637	148.50	384.28	45.65
80	293.520	0.2039	0.5553	147.14	400.66	68.19
81	293.518	0.1953	0.5157	145.49	384.25	74.82
82	293.516	0.1918	0.5447	145.72	413.82	83.41
83	293.514	0.1766	0.5052	142.85	408.73	71.27
84	293.512	0.1748	0.4871	142.09	395.94	70.58
85	293.510	0.1681	0.4921	141.61	414.44	108.47
86	293.508	0.1529	0.4421	137.74	398.16	89.02
87	293.506	0.1545	0.4660	138.06	416.48	67.28
88	293.504	0.1333	0.4187	134.91	423.63	85.95
89	293.502	0.1333	0.4462	135.60	453.69	116.58
90	293.502	0.1217	0.4209	131.72	455.66	110.52
91	293.500	0.1166	0.3829	130.62	428.79	97.48
92	293.498	0.1082	0.3408	128.85	405.95	99.42
93	293.496	0.0963	0.3289	126.46	431.83	142.58
94	293.494	0.0884	0.3130	124.54	441.18	134.78

R_* of the field correlation function and the count rates N_p of the multiplier. The table contains also single scattering intensity data i_{90} with the mean square deviation $\sigma_{i_{90}}$ which have been corrected for turbidity loss and multiple scattering according to eqn. (4). The analysis of i_{90} within the Ornstein–Zernike theory will be given below.

Multiple scattering contributions influence the static as well as the dynamic behavior. This can be seen in Fig. 1, which displays the 3D-cross-correlation functions for the critical sample at two different reduced temperatures $\varepsilon = 2.79 \times 10^{-3}$

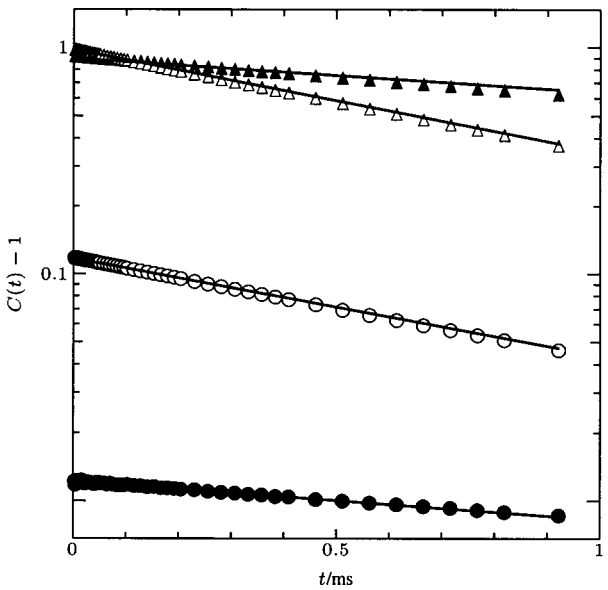

Fig. 1 Cross-correlation (○, ●) and auto-correlation (△, ▲) functions of scattered light intensity at the reduced temperatures $\varepsilon = 2.79 \times 10^{-3}$ (○, △) and $\varepsilon = 6.82 \times 10^{-6}$ (●, ▲) in comparison. These two temperatures correspond to turbidities of $\tau = 0.146$ cm^{-1} and $\tau = 2.43$ cm^{-1}, respectively. The intercept R_τ^2 is a measure for the multiple scattering contribution.

and $\varepsilon = 6.82 \times 10^{-6}$ corresponding to turbidities $\tau = 0.146$ cm^{-1} and $\tau = 2.43$ cm^{-1}, respectively. Both 3D-cross-correlation functions are mono-exponential, as expected for singly scattered light, while the auto-correlation function shows slight systematic deviations from the monoexponential behaviour at the higher turbidity of $\tau = 2.43$ cm^{-1}. Therefore, the analysis of the auto-correlation function would lead to a wrong diffusion constant. While the effect of multiple scattering on the dynamic properties is relatively small, the impact on the static properties, such as the amplitude R_τ, is strong. As can be seen, R_τ gets significantly reduced in the vicinity of the critical temperature at turbidity of $\tau = 2.43$ cm^{-1}. As mentioned above, this is due to an appreciable amount of multiple scattering near T_c where the turbidity of the sample increases strongly. The amount of singly scattered light can be calculated using $R_* = R_\tau/R_{\tau\to 0}$.

The particularly strong influence on the static properties can be confirmed by Monte Carlo simulation.[20,23] The simulation results for the ratio of singly to total scattered light $\langle I_s\rangle/\langle I\rangle$ agree well with the normalized amplitude R_* of the cross-correlation function (see Fig. 2). The input parameters for the simulation were $\tau_0 = 0.496 \times 10^{-4}$ cm^{-1} and $\xi_0 = 0.62$ nm. These values were obtained by a weighted fit of the transmission data to eqn. (5). In agreement with former publications[20] the Monte Carlo simulation results depend strongly on the shape of the spatial aperture. To get a good agreement with the experiment it is necessary to take into account that the width of scattering volume is influenced by the cylindrical shape of the bath. The cylindrical lens effect leads to a width to height ratio of 1 : 1.4. The neglect of the cylindrical contribution affects the simulation result strongly and leads to values of $\langle I_s\rangle/\langle I\rangle$, which are up to 30% above the experimental values, while the scatter of the simulation data is below 1%. The input parameters as shape and dimension of the spatial aperture have to be estimated carefully in order to avoid large systematic errors which easily result in an 8%-error in the amplitude of the correlation length ξ_0. In Fig. 3 we demonstrate the dependence of the light scattering intensity on the reduced temperature. The three curves show the total scattering intensity N_p (▽), the turbidity corrected total intensity $N_p e^{\tau l}$ (△) and the single scattering intensity i_{90} (○) as obtained from the normalized amplitudes of the cross-correlation functions. All three curves agree at reduced temperatures up to 10^{-2} where the turbidity level and multiple scattering contributions are small. The data of N_p pass through a pronounced maximum and cannot be described by the Ornstein–Zernike equation [see eqn. (3)]. If the scattering intensity is corrected for turbidity loss, a description by the Ornstein–Zernike equation leads to systematic deviations close to the critical point. Applying both the turbidity correction and the multiple scattering correction obtained from the amplitudes of the cross-correlation function, the data can be described by the Ornstein–Zernike equation over the entire temperature range with the second set of parameters listed in Table 2. The multiple scattering corrections apply only to reduced temperatures $\varepsilon < 10^{-2}$, as for higher reduced temperatures the experimental scatter of the amplitude of the correlation function is too high to obtain a sustained value of R_*. In the analysis we fixed the Fisher exponent $\eta = 0.032$ to its theoretical value. An independent determination of η is not possible and setting $\eta = 0$ leads to a small variation of the adjusted parameters just barely outside their uncertainties. Treating ν as an adjustable parameter does not improve the result significantly. In another attempt the data have been corrected by the multiple scattering correction determined by the Monte Carlo simulation. The obtained parameters with the critical exponent ν both fixed and as an adjustable parameter are listed in Table 2 as set #5 and #6, respectively. The analyses for the experimental and simulation corrected data agree within their uncertainties. This shows that for the system polystyrene in cyclohexane all deviations from the Ornstein–Zernike behavior which are observed in conventional light scattering experiments[3] can be explained by multiple scattering contributions.

In order to illustrate how strongly multiple scattering obscures the results of the data analysis, we investigate the

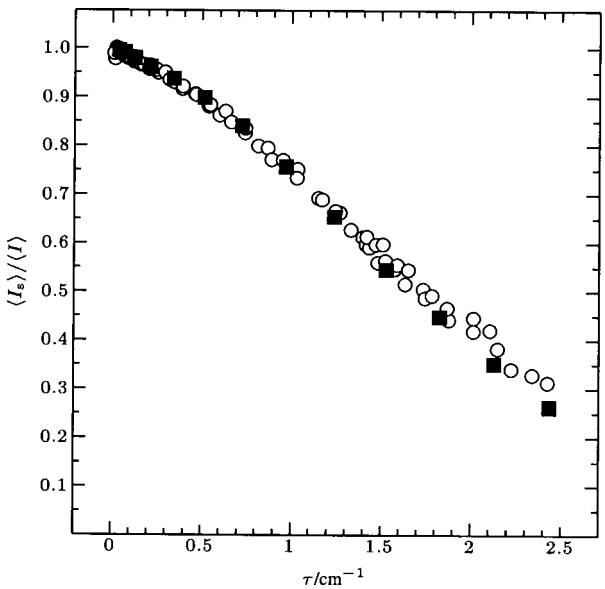

Fig. 2 The ratio of singly scattered light to the totally scattered light $\langle I_s\rangle/\langle I\rangle$ as a function of the turbidity. The circles (○) were determined experimentally from the amplitude R_* of the cross-correlation function and the squares (■) were calculated by Monte Carlo simulation.

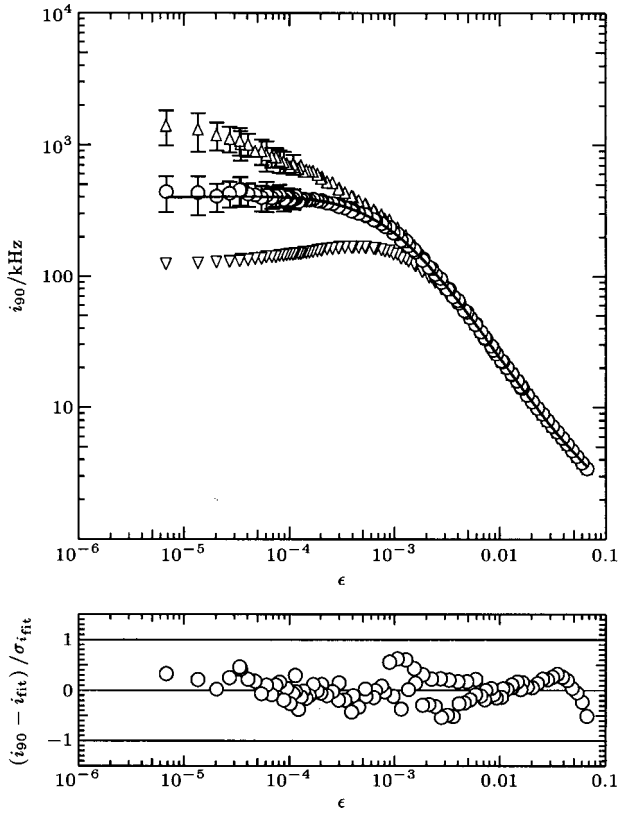

Fig. 3 Light scattering intensity i_{90} *vs.* reduced temperature, and the corresponding deviation plot. The figure shows the uncorrected intensities (▽), the turbidity corrected data (△) and the data (○) which are corrected for multiple scattering using the amplitude R_* of the cross-correlation function. The solid line refers to fit #3 in Table 2. The deviation plot belongs to the same fit result.

Table 2 Results of the fits of the scattering intensities i_{90} to the Ornstein–Zernike equation. For all fits the experimentally observed critical temperature $T_c = 293.492$ K is used. In the first section the turbidity corrected data are used in the analyses where multiple scattering is negligible. Therefore, data points with reduced temperatures below $\varepsilon = 4 \times 10^{-3}$ are excluded from the fit. In the second and third section the data have been corrected for multiple scattering and the complete data set has been used in the analyses. The data have been corrected by the experimentally determined normalized amplitude R_* and the results obtained from the Monte Carlo simulation, respectively.

#	ν	ξ_0/nm	A/kHz	B/kHz	χ^2
Data corrected for turbidity loss					
1	0.630	0.57 ± 0.08	0.079 ± 0.002	1.17 ± 0.18	0.096
2	0.0607 ± 0.052	0.47 ± 0.34	0.096 ± 0.043	0.95 ± 0.56	0.078
Data corrected for turbidity loss and multiple scattering (R_*)					
3	0.630	0.620 ± 0.010	0.0789 ± 0.0013	1.18 ± 0.18	0.061
4	0.623 ± 0.011	0.640 ± 0.035	0.0848 ± 0.0105	1.04 ± 0.29	0.062
Data corrected for turbidty loss and multiple scattering (Monte Carlo)					
5	0.630	0.624 ± 0.008	0.0796 ± 0.0008	1.08 ± 0.14	0.162
6	0.638 ± 0.008	0.602 ± 0.022	0.0728 ± 0.0062	1.25 ± 0.22	0.151

influence of temperature range considered in the fits for N_p, $N_p e^{\tau l}$ and i_{90}. In this survey we keep the critical exponent $\nu = 0.63$ fixed and determine the amplitude ξ_0 of the correlation length. In Fig. 4 we show ξ_0 as a function of the smallest temperature included in the fits. The values of ξ_0 resulting from the fits to the uncorrected data show a pronounced dependence on the temperature range considered. This shows that a determination of ξ_0 from the uncorrected intensities is completely inappropriate. Considering the fits of $N_p e^{\tau l}$ and i_{90} it is noticeable that for $\varepsilon_{min} > 5 \times 10^{-3}$ the resulting values of ξ_0 agree within its naturally very large uncertainty but systematic deviations are noticeable. The deviations between the fits to the two data sets become pronounced when temperatures closer to the critical point are included. Only the fits of i_{90} yield values that are independent of the fitting range. Nevertheless, the dependence of the fits of $N_p e^{\tau l}$ from the included fitting range is rather small and may be difficult to detect if only data from a conventional light scattering experiment are available. The deviation plot shows only a slight systematic and the normalized deviations are below 1%. However, even far from T_c the obtained deviations for ξ_0 lie 10% below the value which is obtained when, in the entire temperature range, the data corrected for multiple scattering are analyzed. Thus even a reduction to data points, which are barely influenced by multiple scattering may lead to parameters that are systematically wrong.

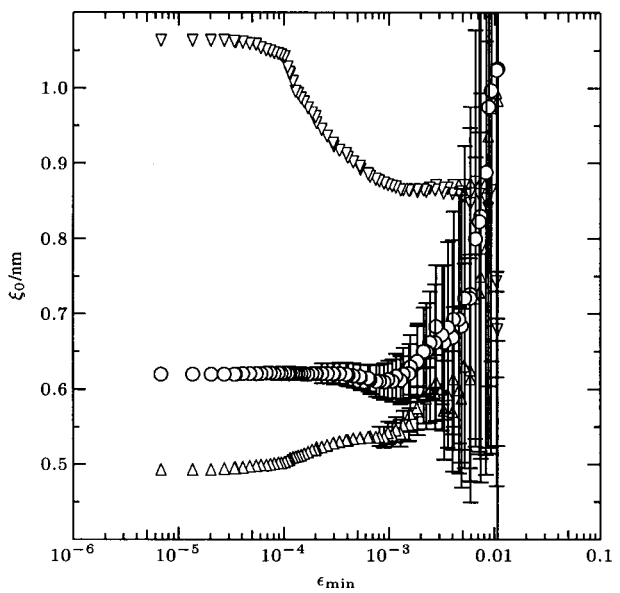

Fig. 4 The adjusted values for the critical amplitude ξ_0 in dependence of the minimal reduced temperature ε_{min} which was included in the fit. The values of ξ_0 determined from the uncorrected intensities (▽), the turbidity corrected intensities (△) and the results for the data corrected for multiple scattering (○). The critical exponent ν was fixed to its theoretical value.

Finally, it can be summarized, that the 3D-cross-correlation technique allows the experimental determination of multiple scattering for temperature-dependent measurements. We show that a variation of the temperature in the range from 20–40 °C done at a scattering angle of 90° requires no realignment of the apparatus. Neglect of the multiple scattering contributions leads to a systematically wrong correlation length amplitude. The comparison between experiment and Monte Carlo simulation gives a complete picture and helps to detect systematic errors. It must be pointed out that the simulation is strongly affected by the scattering geometry and it also depends on a reasonably good estimate of ξ_0 and τ_0. The analysis of the singly scattered light intensity of the critical polystyrene–cyclohexane mixture leads to a correlation length amplitude of $\xi_0 = 0.62 \pm 0.01$ nm. Furthermore, we show that the Ornstein–Zernike function gives a good description of the scattering intensity in the entire temperature range.

Acknowledgements

We thank Thomas Wagner for the synthesis of the polystyrene. The authors thank V. C. Weiss for valuable discussions and advice. We would also like to thank J. Sebald for building the photodiode amplifiers. M. Reichelt built the thermostated cell.

References

1 J. V. Sengers and J. M. H. Levelt Sengers, in *Progress in Liquid Physics*, ed. C. Croxton, John Wiley & Sons, New York, 1978, p. 103.
2 M. E. Fisher, *Rev. Mod. Phys.*, 1998, **70**, 653.
3 R. Kita, K. Kubota and T. Dobashi, *Phys. Rev. E*, 1998, **58**, 793.
4 J. G. Shanks and J. V. Sengers, *Phys. Rev. A*, 1988, **38**, 885.
5 J. K. G. Dhont, *Physica A*, 1983, **120**, 238.
6 J. K. G. Dhont, *Physica A*, 1985, **129**, 374.
7 A. E. Bailey and D. S. Cannell, *Phys. Rev. E*, 1994, **50**, 4853.
8 C. Urban and P. Schurtenberger, *J. Colloid Interface Sci.*, 1998, **207**, 150.
9 L. B. Aberle, P. Hülstede, S. Wiegand, W. Schröer and W. Staude, *Appl. Opt.*, 1998, **37**, 6511.
10 M. Drewel, J. Ahrens and U. Podschus, *J. Opt. Soc. Am. A*, 1990, **7**, 206.
11 E. Overbeck and C. Sinn, *J. Mod. Opt.*, 1999, **46**, 303.
12 W. V. Meyer, D. S. Cannell, A. E. Smart, T. W. Taylor and P. Tin, *Appl. Opt.*, 1997, **36**, 7551.
13 U. Nobbmann, S. W. Jones and B. J. Ackerson, *Appl. Opt.*, 1997, **36**, 7571.
14 G. D. J. Phillies, *Phys. Rev. A*, 1981, **24**, 1939.
15 K. Schätzel, *J. Mod. Opt.*, 1991, **38**, 1849.
16 J. A. Lock, *Appl. Opt.*, 1997, **36**, 7559.
17 V. I. Ovod, *Appl. Opt.*, 1998, **37**, 7856.
18 Th. Engels, L. Belkoura and D. Woermann, *Ber. Bunsen-Ges. Phys. Chem.*, 1988, **92**, 1544.

19 L. B. Aberle, S. Wiegand, W. Schröer and W. Staude, *Progr. Colloid Polym. Sci*., 1997, **104**, 121.
20 L. B. Aberle, M. Kleemeier, P. Hülstede, S. Wiegand, W. Schröer and W. Staude, *J. Phys. D: Appl. Phys*., 1999, **32**, 22.
21 R. F. Chang, H. Burstyn and J. V. Sengers, *Phys. Rev. A*, 1979, **19**, 866.
22 V. G. Puglielli and N. C. Ford, *Phys. Rev. Lett*., 1970, **25**, 143.
23 S. Wiegand, M. E. Briggs, J. M. H. Levelt Sengers, M. Kleemeier and W. Schröer, *J. Chem. Phys*., 1998, **109**, 9038.

Paper 9/02970B